A&A 464, 927–937 (2007)
DOI: 10.1051/0004-6361:20065208

Astronomy & Astrophysics

Na-O anticorrelation and horizontal branches

II. The Na-O anticorrelation in the globular cluster NGC 6752⋆,⋆⋆

E. Carretta[1], A. Bragaglia[1], R. G. Gratton[2], S. Lucatello[2], and Y. Momany[2]

[1] INAF – Osservatorio Astronomico di Bologna, via Ranzani 1, 40127 Bologna, Italy
e-mail: eugenio.carretta@oabo.inaf.it
[2] INAF – Osservatorio Astronomico di Padova, Vicolo dell'Osservatorio 5, 35122 Padova, Italy

Received 15 March 2006 / Accepted 22 December 2006

ABSTRACT

We are studying the Na-O anticorrelation in several globular clusters of different Horizontal Branch (HB) morphology in order to derive a possible relation between (primordial) chemical inhomogeneities and morphological parameters of the cluster population. We used the multifiber spectrograph FLAMES on the ESO Very Large Telescope UT2 and derived atmospheric parameters and elemental abundances of Fe, O and Na for about 150 red giant stars in the Galactic globular cluster NGC 6752. The average metallicity we derive is [Fe/H] = −1.56, in agreement with other results from red giants, but lower than obtained for dwarfs or early subgiants. In NGC 6752 there is not much space for an intrinsic spread in metallicity: on average, the rms scatter in [Fe/H] is 0.037 ± 0.003 dex, while the scatter expected on the basis of the major error sources is 0.039 ± 0.003 dex. The distribution of stars along the Na-O anticorrelation is different to what was found in the first paper of this series for the globular cluster NGC 2808: in NGC 6752 it is skewed toward more Na-poor stars, and it resembles more the one in M 13. Detailed modeling is required to clarify whether this difference may explain the very different distributions of stars along the HB.

Key words. stars: abundances – stars: atmospheres – stars: Population II – Galaxy: globular clusters: general – Galaxy: globular clusters: individual: NGC 6752

1. Introduction

This is the second paper of a series aimed at uncovering and studying the possible existence of a second generation of stars in Galactic Globular Clusters (GCs). As explained in the first paper of the series (Carretta et al. 2006, hereafter Paper I) dedicated to the unusual cluster NGC 2808, to reach our goal we are performing a systematic analysis of a large number of stars (about 100 per cluster) in about 20 GCs, determining accurately and homogeneously abundances of Fe, Na and O. The well known anticorrelation between the abundances of the two last light elements (see Kraft 1994; and Gratton et al. 2004, for reviews covering the early discoveries and recent developments) is attributed to proton-capture reactions in the complete CNO cycle (Ne-Na and Mg-Al chains). The fact that the anticorrelation extends to unevolved stars, unable to mix internal nucleosynthetic products to the surface (Gratton et al. 2001; Ramirez & Cohen 2003; Cohen & Melendez 2005; Carretta et al. 2005) has reinforced the primordial origin hypothesis for these abundance anomalies. If a previous generation of stars has polluted material from which the presently living stars formed, we may expect to see differences in the abundances for those elements involved in nuclear burning in those pristine stars.

D'Antona & Caloi (2004) have suggested that the distribution of stars along the Na-O anticorrelation is related to the distribution of stars along the HB, thus being a potential explanation of the second parameter effect. In fact, He is produced in p-capture at high temperature, the mechanism explaining the Na-O anticorrelation (Denisenkov & Denisenkova 1989; Langer et al. 1993; Prantzos & Charbonnel 2006). Since stars with different He content burn H at different rates, they are expected to have different main sequence lifetimes. At a given age, stars of different masses will be climbing the RGB and, if they loose mass at the same rate, they will end up in different locations along the HB. D'Antona & Caloi (2004) studied a few typical examples, supporting the original hypothesis. In this series we wish to produce a large observational dataset to test this scenario (and other possibilities) in depth.

Since we intend to derive the distribution function of the anticorrelation, not simply the general shape, we require large and unbiased samples of stars in each cluster. In particular, when selecting the targets we do not try to enhance the possibility of including extreme cases in order to define the existence and shape of a (possible) anticorrelation. This was instead what we did when we studied a few turnoff and subgiant branch stars in NGC 6397, 47 Tuc and NGC 6752 itself (Gratton et al. 2001; Carretta et al. 2005), where we selected stars with likely strong or weak CN bands, using the Strömgren c_1 index. A fiber instrument (like FLAMES) mounted at a large telescope (the VLT) is ideal to reach our goal and the homogeneity of data acquisition, treatment and analysis is basic to compare results for different clusters. In fact, our approach is to use the same tools for abundance analysis (the same atomic parameters, the same procedure to derive atmospheric parameters, the same package to reduce spectra and to measure equivalent widths, the same prescriptions for NLTE corrections, the same set of solar reference

⋆ Based on observations collected at ESO telescopes under programme 073.D-0211.

⋆⋆ Full Tables 2, 3 and 5 are only available in electronic form at the CDS via anonymous ftp to
cdsarc.u-strasbg.fr (130.79.128.5) or via
http://cdsweb.u-strasbg.fr/cgi-bin/qcat?J/A+A/464/927

abundances and so on) for a large number of stars in many clusters. We stress that our main target is not simply to uncover the Na-O anticorrelation in several galactic GCs: we currently know that this is as ubiquitous phenomenon (see e.g. Gratton et al. 2004; and Paper I). We intend to use a homogeneous approach in order to get rid of features possibly arising from limited samples and/or not self-consistent analysis; we aim at selecting properties of the Na-O anticorrelation that might be linked to global physical parameters of the GCs, once all the sample of objects available to us will be analyzed.

In this paper we present our results on the Na-O anticorrelation among Red Giant Branch (RGB) stars in NGC 6752. This nearby, low-reddened cluster has been widely studied in the past, although never with the present goal in mind. Its metallicity[1] has been derived from high-resolution spectra by many authors in the range [Fe/H] ~ -1.4 to -1.6 (see e.g., Pritzl et al. 2005, for a recent compilation).

There have also been several studies of the Na-O anticorrelation in NGC 6752 but they have always been based on (much) smaller samples than the one presented here. For instance, Norris & Da Costa (1995) compared Na, O abundances for six giants in this cluster (plus three in NGC 6397, and in 47 Tuc) to the ones in ω Cen, and Yong et al. (2003) studied 20 bright RGB stars. In particular, this is the *first* GC for which a Na-O (and Mg-Al) anticorrelation has been found *also* for unevolved and scarcely evolved stars. Gratton et al. (2001) and Carretta et al. (2005) studied 18 stars near the main sequence Turn-Off and on the subgiant branch, demonstrating that (at least part of) the chemical inhomogeneities in GCs must be implanted in the stars and cannot be explained by evolutionary processes. Deep (or extra) mixing can begin to act only when the star is on the giant branch, after the RGB bump, and cannot work for unevolved stars without deep convective envelopes. This result is also supported by Grundahl et al. (2002), who presented evidence of the Na-O and Mg-Al anticorrelations for giants below the RGB bump; these objects were later reanalyzed by Yong et al. (2005), together with the ones near the RGB tip, for a total of 38 RGB stars. A summary of all the previously available information on the Na-O anticorrelation in this cluster can be found in Carretta et al. (2005); that paper deals mostly with CNO abundances in unevolved stars and presents further arguments in favour of a primordial origin for elemental variations, in particular from an earlier generation of intermediate mass Asymptotic Giant Branch stars (Ventura et al. 2001).

The present paper is organized as follows: an outline of the observations is given in the next section; the derivation of atmospheric parameters and the analysis are discussed in Sect. 3, whereas error estimates are given in Sect. 4. Section 5 is devoted to the intrinsic scatter in Fe, the reddening, and the results for the Na-O anticorrelation; a discussion is presented in Sect. 6 and a summary is given in Sect. 7.

2. Observations and measures

2.1. Observations

Our data were collected (in Service mode) with the ESO high resolution multifiber spectrograph FLAMES/GIRAFFE (Pasquini et al. 2002) mounted on VLT UT2. Observations were done with two GIRAFFE setups, using the high-resolution gratings HR11 (centered at 5728 Å) and HR13 (centered at 6273 Å) to measure the Na doublets at 5682–5688 Å and 6154–6160 Å, and the [O I] forbidden lines at 6300, 6363 Å, respectively. The resolution is $R = 24\,200$ (for HR11) and $R = 22\,500$ (for HR13). We have one single exposure of 1750 s for each grating.

Table 1. Log of the observations for NGC 6752. Date and time are UT, exposure times are in seconds. For both exposures the field center is at RA(2000) = 19:10:51.780, Dec(2000) = −59:58:54.70.

Grating	Date	$UT_{beginning}$	Exptime	Airmass
HR11	2004-06-25	09:54:29	1750	1.787
HR13	2004-06-23	09:41:13	1750	1.677

Our targets were selected among isolated RGB stars, using the photometry by Momany et al. (2004): we chose stars lying near the RGB ridge line without any companion closer than 2″ and brighter than the star magnitude plus 2. Not all the stars were observed with both gratings; on a grand total of 151 different stars observed, we have 72 objects with spectra for both gratings, 41 with only HR11 observations and 38 with only HR13 observations. Since the Na doublet at 6154–6160 Å falls into the spectral range covered by HR13, we could measure Na abundances for all target stars, whereas we could expect to measure O abundances only up to a maximum of 110 stars.

Table 1 lists information about the two pointings, while a list of all observed targets with coordinates, magnitudes and radial velocities (*RV*s) is given in Table 2 (the full table is available only in electronic form at the CDS). The $V, B-V$ colour magnitude diagram (CMD) of our sample is shown in Fig. 1; our targets range from about $V = 11.6$ to 14.6, i.e. from about 1 mag below the RGB tip to about 1 mag below the RGB bump. Two field stars, accidentally included in the sample, are indicated by crosses, and the open star symbol is for a star (49370) whose spectrum presents double lines (due to true binarity or to contamination from a nearby object). These stars are disregarded from the following analysis.

Contamination from AGB stars is not of great concern in our sample. In Fig. 1 the RGB and AGB sequences are clearly separated up to $V, B-V \simeq (11.8, 1.1)$ but very few stars of our sample are located above this point in the CMD. Since AGB stars are expected to be about 10% of RGB stars, contamination from interloper AGB stars should be minimal. This is confirmed, a posteriori, by the very small scatter in the derived abundances, supporting the soundness of the adopted parameters and the attribution of stars to the first ascent red giant branch.

We used the 1-d, wavelength calibrated spectra as reduced by the dedicated GIRAFFE pipeline (BLDRS v0.5.3, written at the Geneva Observatory, see `http://girbldrs.sourceforge.net`). Radial velocities were measured using the GIRAFFE pipeline, which performs cross correlations of the observed spectra with artificial spectral templates. Further analysis was done in IRAF[2]: we subtracted the background using the 10 fibers dedicated to the sky, rectified the spectra and shifted them to zero *RV*. Before this final step, we corrected the HR13 spectra for contamination from telluric features using a synthetic spectrum adapted to our resolution and the intensity of telluric absorption, as we did in Paper I.

There is a very small systematic difference between *RV*s in HR11 and HR13 (on average about 0.3 km s^{-1}, rms 0.05 km s^{-1}), which however has no influence on our abundance analysis. The

[1] We adopt the usual spectroscopic notation, i.e. $[X] = \log(X)_{star} - \log(X)_{\odot}$ for any abundance quantity X, and $\log \epsilon(X) = \log(N_X/N_H) + 12.0$ for absolute number density abundances.

[2] IRAF is distributed by the National Optical Astronomical Observatory, which are operated by the Association of Universities for Research in Astronomy, under contract with the National Science Foundation.

Table 2. List and relevant information for the target stars observed in NGC 6752. ID, *B*, *V* and coordinates (J2000) are taken from Momany et al. (2004); *J*, *K* are from the 2MASS catalog; radial velocities *RV*'s (in km s^{-1}) from both gratings are heliocentric; listed *S/N* values are per pixel, computed from spectra acquired with HR11 when available, else with HR13; stars with "*" in notes have $V-K$ colours that deviate from the ones expected for RGB stars (see text). Stars with "†" in notes have too few lines (being warm and/or of low S/N) to obtain reliable measurements and were dropped from further analysis. The complete table is available electronically at the CDS; we show here a few lines for guidance.

Star	RA (h m s)	Dec (d p s)	*V*	*B*	*J*	*K*	*S/N*	*RV*(HR11)	*RV*(HR13)	HR	Notes
1217	19 12 0.740	–60 0 11.85	13.556	14.383	11.735	11.110	107	–29.52	–29.97	11, 13	
1493	19 11 54.785	–59 59 15.44	13.858	14.643	12.064	11.465	115		–27.22	13	
1584	19 11 52.324	–59 58 52.85	14.241	15.007	12.491	12.065	51	–28.20	–29.17	11, 13	
1797	19 11 46.677	–59 58 8.83	13.791	14.604	12.003	11.442	147		–27.43	13	
2097	19 11 46.252	–59 56 58.97	12.241	13.264	10.108	9.390	253	–22.21	–22.59	11, 13	
2162	19 11 43.044	–59 56 45.39	13.343	14.192	11.433	10.818	117	–25.18	–25.70	11, 13	
2704	19 11 42.883	–59 54 24.53	13.718	14.545	11.897	11.301	81	–25.94	–26.07	11, 13	
2817	19 11 53.262	–59 53 50.04	13.939	14.755	12.166	11.556	76	–26.13	–27.50	11, 13	
3039	19 11 44.832	–59 52 30.49	14.095	14.909	12.347	11.788	41	–29.44		11	†
4602	19 10 41.235	–60 4 36.66	13.778	14.597	11.969	11.384	70	–25.51	–25.79	11, 13	

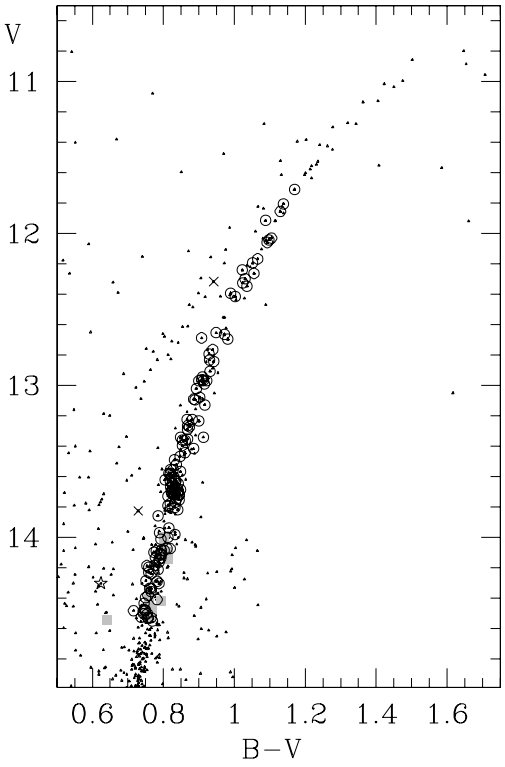

Fig. 1. *V*, $B-V$ CMD for NGC 6752 from Momany et al. (2004; dots); observed stars are indicated by circles. Crosses indicate the two field stars, the open star symbol is for star 49370 whose spectrum shows double lines and filled squares in grey tones indicate warm or faint objects with low S/N spectra and no reliable abundance determinations.

cluster heliocentric average velocity, computed eliminating only two obvious non members, is −25.6 (rms 6.2) km s^{-1}, in good agreement with the value tabulated in the updated web catalog of Harris (1996) and with the average velocity −23.8 ± 2.1 km s^{-1} found from seven stars observed with UVES by Gratton et al. (2005), who also discuss other literature measurements.

2.2. Equivalent widths

Equivalent widths (*EW*s) were measured as described in detail in Bragaglia et al. (2001), adopting a relationship between *EW* and *FWHM* as described at length in that paper. Particular care was devoted to the definition of the local continuum around each line, a delicate task at the moderately limited resolution of our spectra, especially for the coolest targets. The choice of the continuum level is done by an iterative procedure that takes into account only a given fraction of the possible points. After several checks we decided that the optimal choice for NGC 6752 is represented by a fraction of 1 for stars warmer than 4850 K, of 0.7 for stars with $T_{\rm eff}$ between 4600 and 4850 K, and about 0.6 for stars cooler than 4600 K. Note that these values well approximate the general relation that we adopt throughout all this series of papers when analyzing GIRAFFE spectra. A few stars (indicated in Table 2) had too few lines (these objects are warm and/or have low $S/N \leq 60$) to obtain reliable measurements, hence we dropped them from further analysis. Tables of measured *EW*s will be only available at the CDS database.

To check the reliability of *EW*s measured on the GIRAFFE spectra we performed the following steps. While the two GIRAFFE setups were obtained, we also observed 14 RGB stars in NGC 6752 through the dedicated fibers feeding the high resolution ($R \sim 43\,000$) spectrograph UVES. We employed the standard RED580 setup, obtaining spectra in the range 4800–6800 Å[3]. We measured the 8 stars observed both with the GIRAFFE and the UVES configuration with the above procedure; the comparison of the *EW*s is shown in the upper panel of Fig. 2. We found that on average *EW*s from GIRAFFE are larger than those measured from UVES by +7.0 ± 0.7 mÅ (rms = 7.2 mÅ from 114 lines). A linear regression between the two sets of measurements gives $EW_{\rm GIRAFFE} = 1.12(\pm0.02) \times EW_{\rm UVES} + 1.17(\pm0.55)$ mÅ with rms = 5.89 mÅ and a correlation coefficient $r = 0.99$. We inverted this relationship and used it to correct the *EW*s from GIRAFFE spectra to the system of the higher resolution UVES spectra[4].

In the lower panel of Fig. 2 the *EW*s from our UVES spectra are compared with those of two stars in common with the sample by Yong et al. (2003), taken with UVES at the highest possible spectrograph resolution ($R = 110\,000$) and with S/N ranging

[3] The analysis of UVES spectra in NGC 6752 as well as in the other globular clusters studied in the present project will be presented separately.

[4] The difference between the UVES and GIRAFFE *EW*s we found for NGC 6752 spectra is larger than observed for other GCs analyzed in this series. This difference is not simply a function of metallicity. Inspection of the original spectra showed that this difference is not due to the measuring procedure and that lines in spectra of stars at the same position in the CMD may be of different strength. We think that this is due to small but significant effects intrinsic to the GIRAFFE spectra. Our procedure reduces to a minimum the systematic error for each GC.

Table 3. Adopted atmospheric parameters and derived iron abundances in stars of NGC 6752; Nr indicates the number of lines used in the analysis. The complete table is available only in electronic form at the CDS.

Star	$T_{\rm eff}$ (K)	log g (dex)	[A/H] (dex)	$v_{\rm t}$ (km s^{-1})	Nr	[Fe/H]I (dex)	rms	Nr	[Fe/H]II (dex)	rms
1217	4746	2.14	−1.55	1.50	26	−1.54	0.09	3	−1.42	0.09
1493	4821	2.30	−1.55	1.33	16	−1.54	0.07	2	−1.44	0.04
1584	4916	2.48	−1.55	1.41	14	−1.55	0.08	1	−1.47	
1797	4804	2.25	−1.58	1.49	20	−1.57	0.08	2	−1.45	0.01
2097	4418	1.41	−1.59	1.71	39	−1.58	0.09	3	−1.51	0.07
2162	4693	2.02	−1.58	1.52	26	−1.57	0.06	2	−1.52	0.06
2704	4786	2.20	−1.56	1.47	20	−1.55	0.07	3	−1.29	0.08
2817	4841	2.31	−1.61	1.60	22	−1.59	0.11	2	−1.40	0.03
4602	4801	2.24	−1.52	1.33	20	−1.54	0.11	1	−1.57	

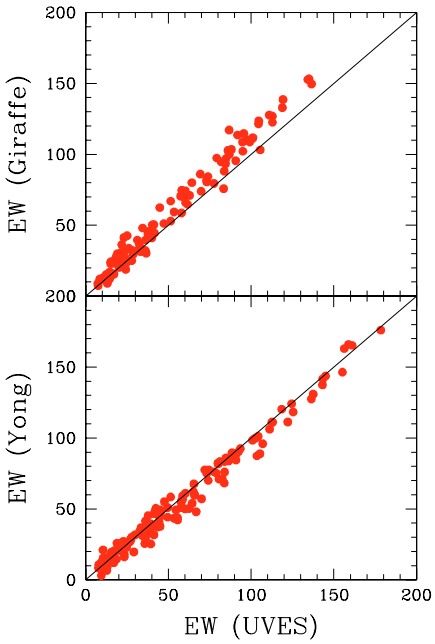

Fig. 2. *Upper panel*: comparison between the *EW*s derived from GIRAFFE and UVES spectra for 8 stars in NGC 6752 observed in both modes. *Lower panel*: comparison between *EW*s from UVES measured for two stars in common with Yong et al. (2003).

from 250 to 150 per pixel. The two stars are 11189, 23999 and mg24, mg15 in our catalogue and in Yong et al. (2003), respectively. The agreement of our measures with their *EW*s, kindly provided by D. Yong (2006, private communication) is excellent: on average the difference (in the sense us minus Yong) is +1.7 ± 0.4 mÅ with σ = 5.6 mÅ from 157 lines. This allows us to be quite confident about errors in the continuum placement being small for the UVES spectra, at a negligible value, lower than 1%[5].

Thus, after correction to the UVES system, the *EW*s measured on the GIRAFFE spectra are not likely to be affected anymore by systematic effects due e.g., to unaccounted blends possibly due to the moderate resolution.

In the following, we analyzed these corrected *EW*s; in the future papers of this series, devoted to other clusters, we plan to check and calibrate our *EW*s by comparison with stars with both UVES and GIRAFFE spectra in a systematic way.

Line lists and atomic parameters for the lines falling in the spectral range covered by gratings HR11 and HR13 are from Gratton et al. (2003b) and are described in Paper I, together with the adopted solar reference abundances. For the interested reader, a more comprehensive discussion of the atomic parameters and sources of oscillator strengths is provided in Sect. 5 and Table 8 of Gratton et al. (2003b).

3. Atmospheric parameters and analysis

3.1. Atmospheric parameters

Temperatures and gravities were derived as described in Paper I; along with the derived atmospheric parameters and iron abundances, they are shown in Table 3 (completely available only in electronic form at the CDS). We used J, K magnitudes taken from the Point Source Catalogue of 2MASS (Skrutskie et al. 2006); the 2MASS photometry was transformed to the TCS photometric system, as used in Alonso et al. (1999).

We obtained $T_{\rm eff}$'s and bolometric corrections B.C. for our stars from $V - K$ colors whenever possible. We employed the relations by Alonso et al. (1999, with the erratum of 2001). We adopted for NGC 6752 a distance modulus of $(m - M)_V = 13.24$, a reddening of $E(B - V) = 0.04$, an input metallicity of [Fe/H] = −1.42[6] (from Gratton et al. 2003a), and the relations $E(V - K) = 2.75E(B - V)$, $A_V = 3.1E(B - V)$, and $A_K = 0.353E(B - V)$ (Cardelli et al. 1989).

The final adopted $T_{\rm eff}$'s were derived from a relation between $T_{\rm eff}$ (from $V - K$ and the Alonso et al. calibration) and V magnitude based on 135 "well behaved" stars (i.e., with magnitudes in all the four filters and lying on the RGB). The assumption behind this procedure is that there is an unique relation between V and $V - K$; this is a sound assumption insofar (i) all stars belong to the RGB; (ii) the RGB is intrinsically extremely thin (i.e. there is no spread in abundances) and (iii) the reddening is the same for all the stars. There is no reason to question the last point for NGC 6752 (the reddening itself is very small, see e.g. Gratton et al. 2003a). The second point can only be verified a posteriori, by looking at the derived abundances. Regarding the first hypothesis, the contamination of stars on the AGB is not of concern in our sample, as discussed in the previous section. This procedure was adopted in order to decrease the scatter in abundances due to uncertainties in temperatures, since magnitudes are much more reliably measured than colours, hence

[5] *EW*s measured on moderate resolution spectra may be either overestimated due to contribution of blends, not recognized when compiling the line list, or underestimated, because the nominal continuum used when extracting *EW*s can be lower than the real value, due to veiling from weak lines, not recognized as such due to the low resolution of the spectrum.

[6] This value is somewhat different from what we derive in the present study (i.e. −1.56), but the dependence of $(V - K)$ on [Fe/H] is so weak that temperatures are unaffected.

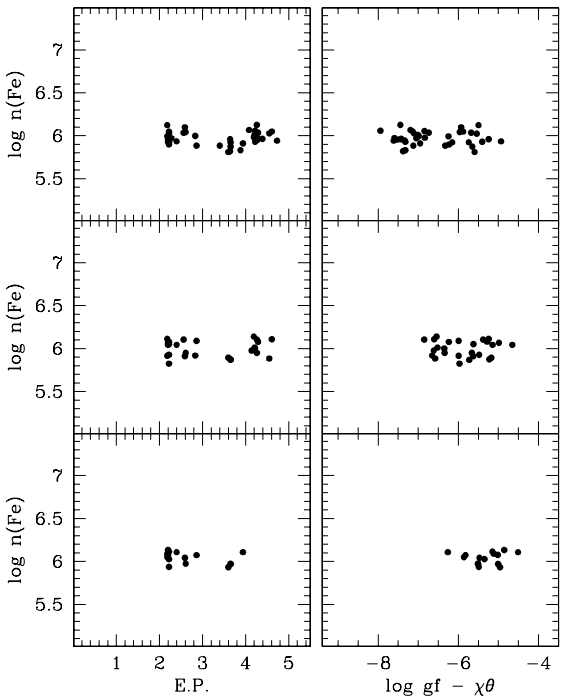

Fig. 3. Abundances deduced from neutral Fe I lines as a function of excitation potential (*left panels*) and of the expected line strength (*right panels*) for three stars on the RGB of NGC 6752: a bright giant (star 48975, $T_{\rm eff}$ = 4337 K, *upper panels*), a star in the middle of our temperature range (star 1217, $T_{\rm eff}$ = 4746 K, *middle panels*) and a faint giant (star 24936, $T_{\rm eff}$ = 4987 K, *lower panels*).

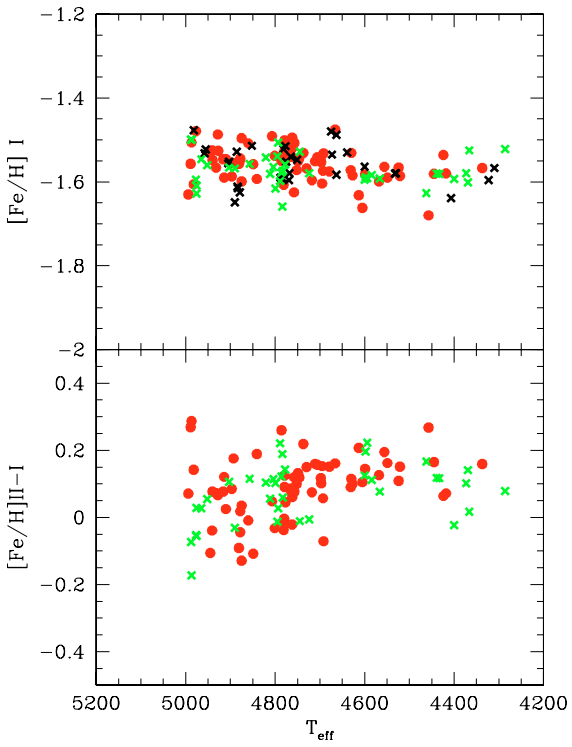

Fig. 4. Run of [Fe/H] ratio and of the iron ionization equilibrium as a function of temperatures for program stars in NGC 6752. Symbols and color coding refer to the setup used: (red) filled circles indicate stars with both HR11 and HR13 observations, (black) crosses for HR11 only, and (green) crosses for HR13 only.

the adopted procedure produces extremely small nominal errors in $T_{\rm eff}$'s, see Sect. 4 below.

Surface gravities log g's were obtained from effective temperatures and bolometric corrections, assuming masses of 0.85 $M_{\odot}$ and $M_{\rm bol,\odot}$ = 4.75 as bolometric magnitude for the Sun.

We obtained values of the microturbulent velocity $v_{\rm t}$ by eliminating trends of the abundances from Fe I lines with *expected* line strength (see Magain 1984). The optimization was done for individual stars; this results in a much smaller scatter in the derived abundances than using a mean relation of $v_{\rm t}$ as a function of temperature or gravity. Concerning stars observed only with the grating HR11, since only a few lines where available, we ended the optimization when the slope of abundances from Fe I lines vs. expected line strength was within 1σ error. Examples of the abundances from neutral Fe lines as a function of the expected line strength and of the excitation potential are shown in Fig. 3 for three stars that cover the entire temperature range of our sample in NGC 6752. Adopted atmospheric parameters are listed in Table 3.

Final metallicities are obtained by choosing by interpolation in the Kurucz (1993) grid of model atmospheres (with the option for overshooting on) the model with the proper atmospheric parameters whose abundance matches that derived from Fe I lines.

Average abundances of iron for NGC 6752 are [Fe/H]I = −1.56 (rms = 0.04 dex, 137 stars) and [Fe/H]II = −1.48 (rms = 0.09 dex, 105 objects). We do not think this difference is really relevant, since abundances for Fe II rely on average on only two lines. Derived Fe abundances are listed in Table 3.

The distribution of the resulting [Fe/H] values and of the difference between ionized and neutral iron are shown in Fig. 4, as a function of temperature, with stars coded according to the grating(s) they were observed with. The (small) scatter of the metallicity distribution is discussed in Sect. 5.

Total errors, computed using only the dominant terms or including all the contributions (see Sect. 4), are reported in Table 4, in Cols. 8 and 9 respectively. They were scaled down by weighting the sensitivity abundance/parameter with the actual internal error in each parameter.

As already mentioned in the Introduction, the metallicity of NGC 6752 has been determined by several other authors. Limiting to very recent papers that analyzed UVES spectra of resolution higher (R = 45 000) or even much higher (R = 60 000 or 110 000) than ours, we cite: Gratton et al. (2001), based on spectra of main sequence and subgiant branch stars ([Fe/H] = −1.42); Gratton et al. (2005), based on FLAMES/UVES spectra of 7 RGB stars near to the RGB bump ([Fe/H]I = −1.48, [Fe/H]II = −1.55); Yong et al. (2005), based on very high resolution spectra of 38 RGB stars ([Fe/H] = −1.61). A detailed comparison with literature results would require to understand all the systematics between different analyses (e.g., temperature scale, model atmospheres, etc.) and is completely outside the scope of the present paper. Overall, if we limit ourselves to red giants the agreement is excellent, showing the reliability of iron abundances derived from relatively low resolution spectra as those from the GIRAFFE/MEDUSA instrument, once they are checked and calibrated on the scale of *EW*s derived from the higher resolution UVES spectra using stars observed in both modes. The difference is larger when abundances derived from dwarfs and early subgiants are considered. While part of this difference can be related to the different line subset used in the analyses, it is possible that the discrepancy is caused by systematic differences in the atmospheres of dwarfs and giants with respect to the models by Kurucz.

Table 4. Sensitivities of abundance ratios to variations in the atmospheric parameters and to errors in the equivalent widths, as computed for a typical program star with $T_{\rm eff} \sim 4750$ K. The total error is computed as the quadratic sum of the three dominant sources of error, $T_{\rm eff}$, $v_{\rm t}$ and errors in the *EW*s, scaled to the actual errors as described in the text (Col. 8: tot.1) or as the sum of all contributions (Col. 9: tot.2).

Ratio	$\Delta T_{\rm eff}$ (+50 K)	$\Delta \log g$ (+0.2 dex)	Δ [A/H] (+0.10 dex)	$\Delta v_{\rm t}$ (+0.10 km s^{-1})	$\langle N_{\rm lines} \rangle$	$\Delta\, EW$	tot.1 (dex)	tot.2 (dex)
(1)	(2)	(3)	(4)	(5)	(6)	(7)	(8)	(9)
[Fe/H]I	+0.063	−0.007	−0.009	−0.025	23	+0.020	0.039	0.039
[Fe/H]II	−0.024	+0.085	+0.023	−0.010	2	+0.068	0.069	0.070
[O/Fe]	−0.046	+0.088	+0.026	+0.023	1	+0.096	0.101	0.102
[Na/Fe]	−0.023	−0.029	−0.004	+0.018	3	+0.055	0.060	0.060

4. Errors in the atmospheric parameters

In this section we will consider possible analysis errors leading to an increase in the scatter of the relations used throughout this paper. We leave aside errors arising from the simplification in the analysis (1-d plane-parallel model atmospheres, LTE approximation etc.). These errors are relevant when comparing abundances of stars in different evolutionary phases and with different atmospheric parameters (see e.g., Asplund 2005); this might possibly be an explanation of the differences between abundances for dwarfs and red giants, which appears to be rather large and significant. However, we expect such errors to show up as trends in the derived abundances, rather than in scatter at a given location in the color–magnitude diagram. Possibly, such errors might be responsible, e.g., for the systematic trend for the coolest stars to produce lower values of the Fe abundances from neutral lines. However, this effect is small within the range of temperatures (from 5000 to 4300 K) considered here.

Errors in the derived abundances are mainly due to three main sources, i.e. errors in temperatures, in microturbulent velocities and in the measurements of *EW*s. Less severe are the effects of errors in surface gravities and in the adopted model metallicity. As in Paper I, in the following we will concentrate on the major error sources.

Errors in temperatures. The final derivation of temperatures in NGC 6752 slightly differs from the procedure adopted for NGC 2808 (Paper I). There is no evidence of differential reddening in NGC 6752, hence for the stars in the present sample we adopted a final $T_{\rm eff}$ value from a calibration of temperature as a function of the V magnitude. This approach might not be the best for the coolest stars (namely those with $T_{\rm eff} < 4500$ K), where some degree of variability in magnitude may be expected, due to the small number of ascending convective cells in the atmosphere. However, this effect should be amply compensated by the increase of the S/N ratio.

The nominal internal error in $T_{\rm eff}$ is estimated from the adopted error of 0.02 mag in V (a conservative estimate, very likely overestimated, in this magnitude range, where photometric errors are less than a few thousandths of magnitude, see Momany et al. 2004) and the slope of the relation between temperature and magnitude. In NGC 6752 this slope is on average 248 K/mag, hence the conservative estimate of the star-to-star errors in the V magnitude of 0.02 mag produces an internal error as low as 5 K. Of course, systematic and in particular scale errors might be considerably larger. We want to stress here that this is the error relevant when we intend to study a star-to-star variation in some elemental abundances in a single cluster, as is the present case for the Na-O anticorrelation (see below for a discussion of the meaning we attribute to these small errors).

Errors in microturbulent velocities. We used star 1217 and repeated the analysis changing $v_{\rm t}$ until the 1σ value[7] from the original slope of the relation between line strengths and abundances was reached; the corresponding internal error is 0.13 km s^{-1}. This quantity is larger than the one we found for NGC 2808 (Paper I: 0.09 km s^{-1}), since it depends on the position of the measured lines along the curve-of-growth: in NGC 6752 we measured a smaller number of lines, which are moreover weaker, hence less sensitive to the microturbulence. The scatter in individual microturbulent velocities along a mean regression line with gravity (or effective temperature) is of 0.17 km s^{-1} (stars with more than 15 lines measured) or 0.21 km s^{-1} (all stars). Scatter in Fe abundances are reduced when adopting individual values, with respect to the result obtained using the mean line. This strongly suggests that this scatter reflects a real characteristic of the atmospheres, rather than simply an observational error. On the other hand, the physical interpretation of the "microturbulent velocity" in an analysis like ours is not straightforward. While it might indicate the velocity fields in the stellar atmosphere, it might also be related to a different (average) dependence of the temperature on the optical depth, since microturbulent velocities are derived by eliminating trends in abundances with line strength rather than by fitting line profiles (a procedure that would however be meaningless at the resolution of our spectra). Hence, the most correct interpretation of the observed scatter in the microturbulent velocities is that the atmosphere of each star has its own differences with respect to the average model atmosphere, either in the velocity field, or in the thermic structure, or both. It is also possible that these differences change with time, and that a spectrum obtained at a different epoch for the same star would be interpreted with a different microturbulent velocity. This is in fact what should be expected if convection is a time-variable phenomenon, as expected by 3-d model atmospheres (see Asplund 2005) taking into account the large size of the convective cells in the atmospheres of red giants. On this respect, the very small nominal error we obtained for the effective temperatures should not be overinterpreted.

Errors in measurement of equivalent widths. Errors in the individual *EW*s may be estimated by comparing the *EW*s measured in couples of stars with very similar atmospheric parameters and *S/N* ratios, and computing the rms scatter about the linear relationship between the two stars. Assuming that both sets of *EW*s have equal errors, we may estimate the typical internal errors in *EW*s. We applied this procedure to pairs of stars over all the temperature range of our sample. Typical average measurement errors of 3.7 mÅ were derived, yielding typical line-to-line

[7] This value was derived as the quadratic mean of the 1σ errors in the slope of the relation between abundance and expected line strength for all stars with more than 15 lines measured.

scatter in abundances of 0.096 dex for Fe I (this is the quadratic mean over 92 stars with more than 15 measured Fe lines). The contribution of random errors in the *EW*s to errors in the abundances can then be obtained by dividing this typical errors for individual lines by the square root of the typical number of lines used in the analysis (22), providing a typical internal error of 0.020 dex.

Once we have derived the internal errors we may compute the final errors in abundances; they depend on the slopes of the relations between the variation in each given parameter and the abundance. Columns from 2 to 5 of Table 4 show the sensitivity of the derived abundances to variations in the adopted atmospheric parameters for Fe, Na and O. This has been obtained by re-iterating the analysis while varying each time only one of the parameters of the amount shown in the Table. This exercise was done for all stars in the sample. The average value of the slope corresponding to the average temperature (~4750 K) in the sample was used as representative to estimate the internal errors in abundances, according to the actual uncertainties estimated in the atmospheric parameters. For iron, these amount to ~0.01 dex and 0.033 dex, due to the quoted uncertainties of 5 K and 0.13 km s^{-1} in $T_{\rm eff}$ and $v_{\rm t}$. The impact of errors in *EW*s is evaluated in Col. 7, where the average error from a single line is weighted by the square root of the mean number of lines, given in Col. 6. This has been done for iron and for the other two elements measured in this paper. Of course this approach corresponds to an interpretation of the variation of microturbulence as due to real velocity fields in the stellar atmosphere, and to the adoption of the nominal values for the errors in the effective temperatures. While the above discussion shows that this interpretation may be incorrect, we notice that the good agreement with the actual scatter in Fe abundances (see next section) suggests that the total (internal) error given by this interpretation is not grossly wrong.

5. Results

5.1. Cosmic scatter and reddening

To evaluate the expected scatter in [Fe/H] due to the uncertainties in $T_{\rm eff}$, $v_{\rm t}$ and errors in *EW*s we make use of Table 4; we derive $\sigma_{\rm FeI}$(exp.) = 0.039 ± 0.003 dex (statistical error). The inclusion of contributions due to uncertainties in surface gravity or model metallicity does not alter our conclusions. The observed scatter, estimated as the average rms scatter that we obtain using the 92 stars in our sample with at least 15 measured iron lines, after a 3σ clipping, is formally lower: $\sigma_{\rm FeI}$(obs.) = 0.037 ± 0.003 (statistical error). However, within the statistical uncertainties this difference is not significant, and might indicate that the errors are slightly overestimated. The conclusion from our large dataset is that the observed star-to-star rms scatter in Fe abundances in NGC 6752 is no more than 9% (decreasing to 8% had we adopted a more tight clipping at 2.5σ).

This is the second cluster of our sample and we can check that we are obtaining results as homogeneous as possible. One can worry e.g., about the fact that we are deriving $T_{\rm eff}$'s and $\log g$'s from the photometry using reddening values and distances coming from different sources for individual clusters.

Distance has a direct impact on $\log g$, but reasonable systematic errors on it (of the order of 0.2 mag in distance modulus) translate into a difference of less than 0.1 in $\log g$, which is negligible, at least for Fe I (see Table 4). An even more negligible effect is produced by systematic differences in the reddening scales between the two analyses.

On the contrary, the influence of diverse reddening scales on the temperatures is noticeable: a systematic shift of 0.02 mag means $T_{\rm eff}$'s from $V-K$ differing by about 40 K, or Fe I abundances differing by about 0.05 dex. We may estimate the consistency of the reddening values adopted in the two cases (0.22 and 0.04 for NGC 2808 and NGC 6752, respectively) comparing two different temperatures scales, one dependent from the reddening ($T_{\rm eff}$'s derived from the photometry) and one independent from it ($T_{\rm eff}$'s derived from the line excitation equilibrium). Let $\Delta\theta = \Delta({\rm FeI}/EP)$ be the slope of the relation between abundances from neutral iron lines and excitation potential; we can derive a relation between $\Delta\theta$ and the photometric temperature, and we obtain that for temperatures (based on $V-K$) of about 4500 K, a difference of 45 K corresponds to $\Delta\theta$ = 0.013 dex/eV. The model atmospheres and the oscillator strengths used in the two analyses are the same, so they do not introduce differences; if the reddenings are on the same scale, the average $\Delta\theta$'s for the two clusters should have to be the same. We chose only stars with enough measured lines to derive $T_{\rm eff}$ spectroscopically, i.e. those with >25 lines in NGC 2808 (there are 63) and >15 lines in NGC 6752 (there are 92), obtaining $\langle\Delta\theta\rangle(2808) = -0.009 \pm 0.003$ (rms = 0.026) and $\langle\Delta\theta\rangle(6752) = -0.006 \pm 0.003$ (rms = 0.026). Given the above dependence of $\Delta\theta$ on $T_{\rm eff}$, the difference in $\Delta\theta$'s between the two clusters (-0.003 ± 0.004) corresponds to −10 K, or −0.004 mag in $E(B-V)$. Furthermore, 10 K correspond to slightly more than 0.01 dex in Fe I.

We may safely assume that the two reddening values and metallicities are on a consistent scale.

5.2. The Na-O anticorrelation

Abundances of O and Na rest on measured *EW*s (or upper limits). Abundances of Na could be measured for all stars; depending on the setup used, at least one of the Na I doublets at 5672–88 Å and at 6154–60 Å is always available. Derived average Na abundances were corrected for effects of departures from the LTE assumption using the prescriptions by Gratton et al. (1999).

Oxygen abundances are obtained from the forbidden [O I] lines at 6300.3 and 6363.8 Å; the former was cleaned from telluric contamination by H_2O and O_2 lines before extracting the *EW*.

CO formation is not a source of concern in the derivation of O abundances due to the low expected C abundances and to the rather high temperatures of these stars. Also, as in Paper I, we checked that the high excitation Ni I line at 6300.34 Å is not a substantial contaminant, giving a negligible contribution to the measured *EW*s of the forbidden [O I] line.

Abundances of O and Na are listed in Table 5 (the complete table is available only in electronic form at the CDS). For O we distinguish between actual detections and upper limits; for Na we also indicate the number of measured lines and the rms value.

The [Na/Fe] ratio as a function of [O/Fe] ratio is displayed (filled dots) in the upper panel of Fig. 5 for each of the red giant stars with both O and Na detections in NGC 6752; stars in which only upper limits in the *EW*s of the [O I] 6300 Å line were measured are also shown as arrows. Despite the moderately high resolution and relatively high *S/N* ratios of our spectra we were not able to reach down to [O/Fe] ~ −1, at variance with NGC 2808 (Paper I) where we measured such low abundances, thanks to the high quality of the spectra and to the higher cluster metallicity.

However, from our study alone we cannot completely exclude that a few very O-poor stars are also present in this cluster.

Table 5. Abundances of O and Na in NGC 6752. [Na/Fe] values are corrected for departures from LTE. HR is a flag for the grating used (1 = HR13 only, 2 = HR11 and HR13, 3 = HR11 only) and lim is a flag discriminating between real detections and upper limits in the O measurements (0 = upper limit, 1 = detection). The complete table is available only in electronic form at the CDS.

Star	Nr	[O/Fe]	rms	Nr	[Na/Fe]	rms	HR	lim
1217	1	+0.01		4	+0.72	0.07	2	0
1493	1	+0.02		2	+0.36	0.09	1	0
1584	1	+0.29		2	+0.14	0.08	2	0
1797	1	+0.01		2	+0.42	0.09	1	0
2097	2	−0.01	0.03	3	+0.84	0.05	2	1
2162	1	+0.10		4	+0.57	0.06	2	0
2704	1	+0.58		3	+0.26	0.05	2	1
2817	1	+0.62		3	+0.37	0.14	2	1
4602	1	−0.01		3	+0.51	0.11	2	0
4625	1	+0.47		2	−0.05	0.10	2	1
4787	1	+0.11		3	+0.65	0.05	2	0

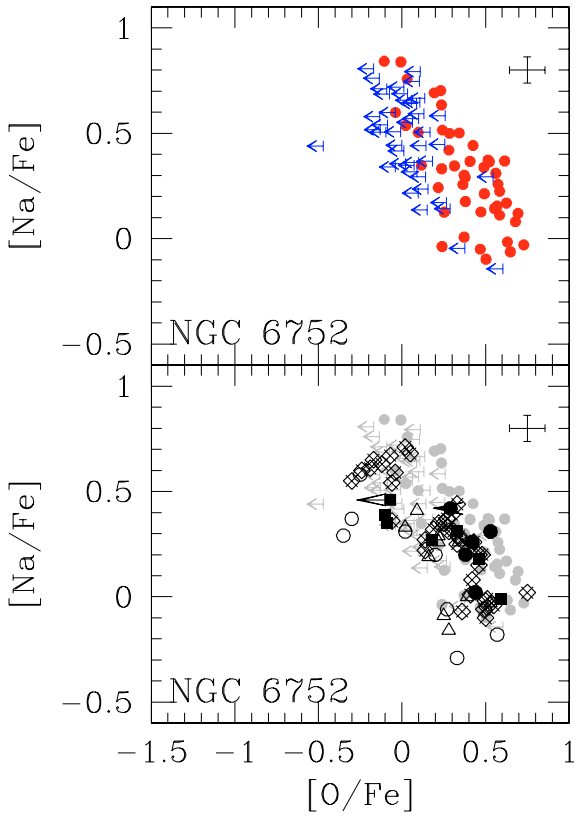

Fig. 5. *Upper panel*: [Na/Fe] ratio as a function of [O/Fe] for red giant stars in NGC 6752 from the present study. Upper limits in [O/Fe] are indicated as blue arrows. The error bars take into account the uncertainties in atmospheric parameters and *EW*s. *Lower panel*: literature data from several study (see text) superimposed to our results. Filled and open large circles are subgiant and turnoff stars from Gratton et al. (2001) and Carretta et al. (2004). Filled squares are RGB stars from Gratton et al. (2005). Diamonds with crosses inside are RGB stars from Yong et al. (2003, 2005). Open triangles are giants from Norris & Da Costa (1995) and Carretta (1994).

A possible example is provided by star 30433, for which we only derived an upper limit [O/Fe] < ∼−0.5 dex. In Fig. 6 we show the spectral region including the forbidden [O I] 6300.31 Å line for this star, compared to the same region star 2097, with very similar atmospheric parameters. For star 2097 (with an estimated $S/N \sim 250$) we actually measured an *EW* whereas only

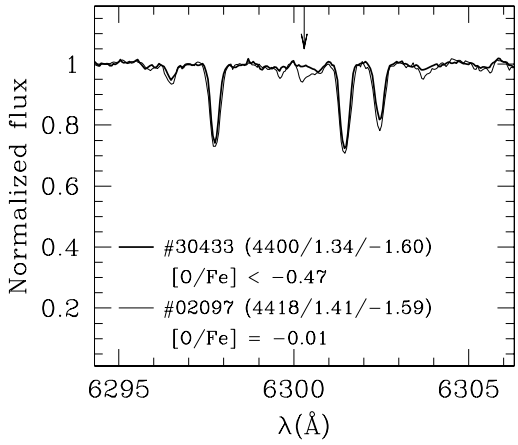

Fig. 6. Comparison of the observed spectra of stars 30433 and 2097 in NGC 6752 near the [O I] 6300.31 Å line. These stars have very similar atmospheric parameters ($T_{\rm eff}$, $\log g$ and [Fe/H] are indicated), yet quite different [O/Fe] abundances.

a conservative upper limit can be safely derived for star 30433. Notice that the estimated S/N ratio for this latter is about 135 per pixel, hence we are quite confidant that the lack of measurable features at 6300 Å is real.

However, the overall impression is that stars with very low O abundances ([O/Fe] < −0.5 dex) are quite scarce in this cluster, if any. This conclusion is supported by the comparison with other literature results for NGC 6752, shown in the lower panel of Fig. 5. In this panel we superimposed to the present data O and Na abundances from a number of studies, derived both from giants and unevolved stars (from Gratton et al. 2001 and Carretta et al. 2004 for subgiant and dwarf stars; from Gratton et al. 2005; Yong et al. 2003, 2005; Norris & Da Costa 1995; and Carretta 1994, for RGB stars). The agreement with previous analyses is very good. All these studies are based on high resolution spectra, and in none of these an extremely O-poor star is present, not even in the dataset by Yong et al. (2003, 2005), where very high *S/N* values (up to 300–400) are obtained.

NGC 6752 seems in this respect more similar to the majority of GCs (see Fig. 5 in Paper I) where the bulk of measured [O/Fe] ratios is in the range +0.5 to −0.5.

The distribution function of stars along the Na-O anticorrelation in NGC 6752 is shown in the upper panel of Fig. 7, where the ratio [O/Na] from our data is used. The dashed area shows the distribution obtained by using only actual detections or carefully checked upper limits. The empty histogram is derived by following the overall Na-O anticorrelation, as derived in Paper I from a collection of literature data and NGC 2808, in order to estimate [O/Fe] values even for stars with no observations in HR13.

The middle and lower panels of Fig. 7 show the distribution functions for stars brighter and fainter than the magnitude level of the RGB-bump (V = 13.65, estimated from the photometry by Momany et al. 2004; the bump is also clearly visible in Fig. 1). From a Kolmogorov-Smirnov statistical test the two distributions may be extracted from the same parent distribution. The magnitude of the bump on the RGB marks the evolutionary point where a second phenomenon of mixing ("extra-mixing") is allowed to onset in Population II red giants (see Gratton et al. 2000, for a detailed discussion and references). Our results, based on the largest sample ever studied with homogeneous procedures in this cluster, strongly support the conclusion that in NGC 6752 the bulk of chemical anomalies in Na and

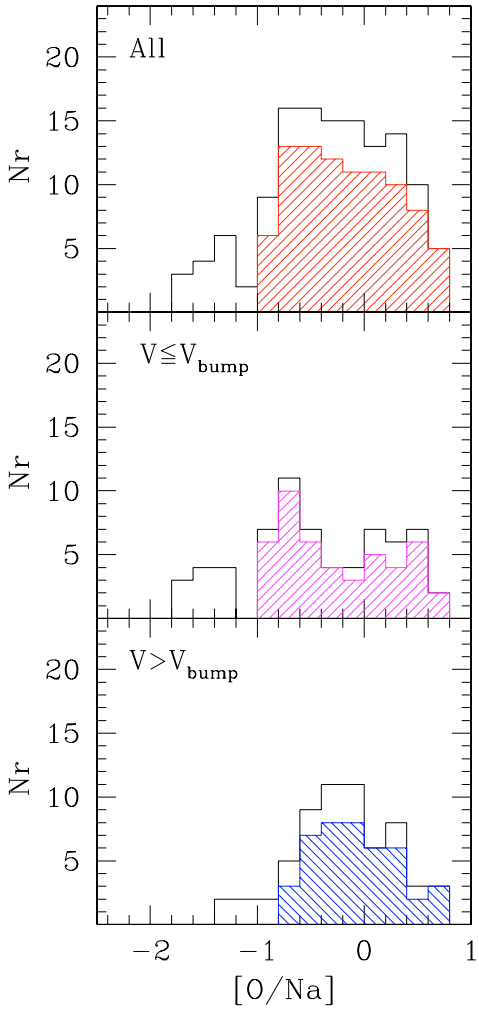

Fig. 7. *Upper panel*: distribution function of the [O/Na] ratios along the Na-O anticorrelation in NGC 6752. The dashed area is the frequency histogram referred to actual detection of O in stars, whereas the empty histogram is obtained by using the global anticorrelation relationship derived in Paper I to obtain O abundances also for stars with no observation with HR13. *Middle and lower panel*: the same, for stars brighter and fainter than the magnitude of the RGB-bump in NGC 6752 (V = 13.65), respectively.

O abundances is primordial, already established in stars before any evolutionary mixing is allowed. Any further modification in the [Na/Fe] or [O/Fe] ratios due to mixing mechanisms during the evolution along the RGB must be considered as a second order effect.

6. Discussion

The first conclusion of our study is that in NGC 6752 there is no measurable intrinsic spread in metallicity, and that this cluster is very homogeneous as far as the global metallicity is concerned. In turn, this result emphasizes that every model proposed to explain the formation of a globular cluster has to face very tight constraints. Abundance anomalies and anticorrelations between elements forged in high temperature p-capture reactions are likely the relics of ejecta from intermediate-mass AGB stars[8]. On the other hand, iron is not produced in such stars, but mainly in more massive stars exploding early as core-collapse supernovae. We might expect that the proto-GCs might have been able to have some independent chemical evolution, retaining at least part of the metal-enriched ejecta of core-collapse SNe (Cayrel 1986; Brown et al. 1991, 1995; Parmentier & Gilmore 2001). Considering the typical mass of a globular cluster (likely larger in the past, due to possible stripping and evaporation of stars) some tens of supernovae are presumably required in order to enrich the whole protocluster. Thus, a physically realistic model *must* include a very efficient (turbulent?) mixing of the protocluster cloud, in order to match the very homogeneous metallicity of the observed stars in NGC 6752.

The second item to be considered concerns the Na-O anticorrelation. We have currently available 2 GCs with much more than 100 stars observed and analyzed in a very homogeneous way (the largest samples ever used to study in detail the Na-O anticorrelation). Therefore, it is tempting to draw some preliminary inferences from our datasets. When coupled with other literature data, some simple statements are already possible. In fact, we know that:

(i) as Sneden et al. (2004) pointed out, red giants in NGC 6752 and M 13 share the same anticorrelation between [O/Fe] and the same relative ratio of the Mg isotopes. On the other hand, the excellent study by Yong et al. (2003) in NGC 6752 shows that the source of the Mg isotopes is likely a generation of intermediate mass stars in the range 3–6 $M_{\odot}$, confirming the earlier findings by Gratton et al. (2001) from the abundance analysis of unevolved stars in this cluster.
(ii) the comparison between NGC 6752 and M 13 seems to imply that the latter suffered a greater degree of pollution than the former.
(iii) the HB morphology in NGC 6752 and M 13 is similar: the horizontal-branch ratio, HBR = $(B-R)/(B+V+R)$, is 0.97 for M 13 and 1.0 for NGC 6752, meaning that both M 13 and NGC 6752 have blue HBs, with stars populating only the region hotter than the RR Lyrae instability strip;
(iv) large degree of anomalies as in O, Mg depletion and Na, Al enhancement are observed also in NGC 2808 (Paper I and Carretta 2006), and they are as extreme as those found in M 13; yet, the HBR parameter is −0.49 for NGC 2808, which represents a more complicate case (Paper I and literature there cited);
(v) however, Carretta (2006) convincingly showed that no correlation seems to be present between the extension of both the Na-O and Mg-Al anticorrelations and the HB morphology.

Figure 8 compares the results obtained from our large datasets in NGC 6752 and NGC 2808. The distribution functions look somewhat different; the Kolmogorov-Smirnov statistic returns a probability of only about 7% that the two subsamples are extracted from the same parent population. The distribution of stars along the [O/Na] anticorrelation in NGC 6752 is more similar to the one for M 13 than to the NGC 2808 one (see Fig. 7 in Paper I). Although no super O-poor stars are found in the present study or in any other published to date, there is still the possibility that NGC 6752 could host a handful of such stars. In the moderately limited sample by Yong et al. (2003, 2005), where the O abundances are all detections based on high quality spectra,

[8] Very recently, Prantzos & Charbonnel (2006) suggested instead that the Na-O anticorrelation is due to nucleosynthesis in rapidly rotating massive stars rather than in AGB stars. While this difference would not affect most of the present discussion, we note that the very small scatter in Fe abundances sets stringent limits on the "inefficiency" of mixing between the slow winds of stars in the supergiant phases and the ejecta from core-collapse supernovae in this scenario.

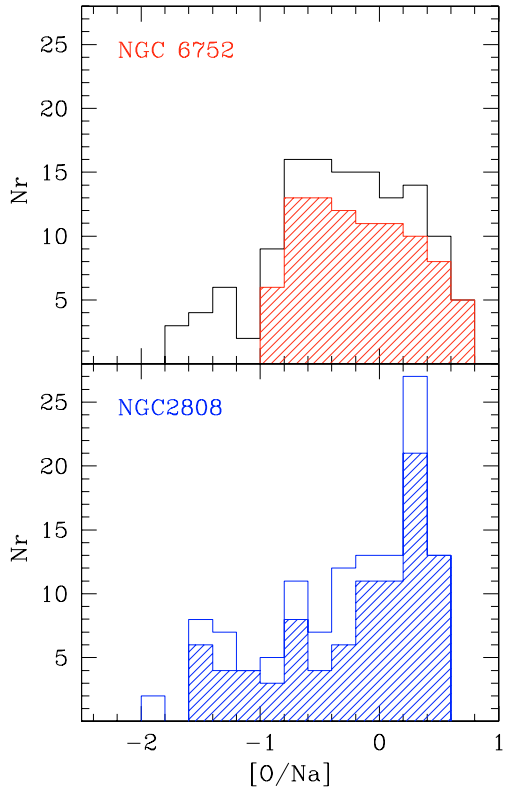

Fig. 8. Comparison of the distribution functions of the [O/Na] ratios for stars along the red giant branches in NGC 6752 (*upper panel*, this work) and in NGC 2808 (*lower panel*, Carretta et al. 2006).

there are no super O-poor stars out of 38 objects: according to the binomial distribution, at 95% level of confidence a firm upper limit to the population of extremely O-poor stars in NGC 6752 is 8%. Regarding our much larger sample, this estimate is more uncertain, due to the upper limits in the [O/Fe] ratios; however, the results are not at odds with those by Yong et al.

These findings emphasize a potential inconsistency in the scenario proposed e.g. by D'Antona & Caloi (2004): if the progeny of super O-poor stars on the RGB is located on the bluest part of the HB (EBHB), we should expect that less than about 8% of the horizontal branch stars in NGC 6752 populate this region of the HB. However, the populous blue tail of the HB in this cluster contains at least about 20% of HB stars, implying a discrepancy of about a factor of 2. A possible way out is if most of EHB's are the outcome of binary star evolution; however, this is at odds with results by Moni Bidin et al. (2006) who detected no close binary system among 51 hot HB stars. Moreover, in NGC 6752 also the progeny of "normal", O-rich stars is confined to the blue HB only. A detailed modeling and fine tuning of the mass loss process would be required to reproduce the HB distribution in this cluster.

Another possibility is that we are seeing less stars on the RGB than expected, in particular those with extremely low O abundances, because they never reach the upper part of the giant branch: these objects could maybe loose a large amount of mass, becoming RGB-manquè and ending up on the EBHB. This hypothesis can be checked using number counts of stars populating different parts of the CMD (RGB, HB) that should be clearly affected. In particular, the R parameter, usually employed to determine the helium abundance (e.g. Buzzoni et al. 1983) is based on the the ratio of HB to RGB stars. Interestingly enough, the latest compilation of R parameters by Sandquist (2000) shows that several clusters with the bluest HB morphologies have unusually high R values, NGC 6752 among these. Unfortunately, nothing conclusive can be derived from the presently extant data: Sandquist reports a value $R = 1.56 \pm 0.18$ based on the rather old photographic photometry by Buonanno et al. (1986). Thus the R parameter goes in the right direction, being able to explain the excess of about 12% of stars in the blue tail required to reconcile the numbers of RGB-manquè and HB stars, since it is about 12% larger in this cluster, with respect to the average of other GCs. However, the attached error is currently still too high (it is itself about 12%) and precludes a firmer conclusion.

Finally, we note here that NGC 6752 and M 13 have similar metallicities, while NGC 2808 is slightly more metal-rich; the latter is also younger (Rosenberg et al. 1999) than the bulk of GCs. For NGC 6752 the HB populated only in the blue part must be mostly due to the influence of the first parameter (metallicity) and maybe to the age.

Further discussion is obviously postponed until a substantial fraction of our sample of GCs, with different HB morphologies, has been studied, but the emerging scenario is a rather complex one where several factors (excess of He from a prior generation of stars, age, metallicity) may contribute to build up both the final Na-O anticorrelation on the RGB and the star distribution on the HB. The relative weight of these contributions, as well as the global properties such as the cluster orbital parameters (see Carretta 2006), may then compete to give the observed differences in individual objects.

7. Summary

In this paper we have derived atmospheric parameters and elemental abundances for about 150 red giant stars in the globular cluster NGC 6752 observed with the multifiber spectrograph FLAMES.

Atmospheric parameters for all targets were obtained from the photometry. From the analysis of the GIRAFFE spectra we derived an average metallicity [Fe/H] = −1.56 (rms = 0.04 dex, 137 stars), without indication of intrinsic star-to-star scatter.

From the forbidden [O I] lines at 6300.3, 6363.8 Å and the Na doublets at 5682–88 and 6154–60 Å we measured O and Na abundances for a large sample of stars. The [Na/Fe] versus [O/Fe] ratios follow the well known Na-O anticorrelation, signature of proton-capture reactions at high temperature, found in all other GCs examined so far. The anticorrelation in NGC 6752 is the same at every luminosity along the RGB, suggesting that any mixing effect must be negligible.

We also derived the distribution function of stars in [O/Na], i.e. along the Na-O anticorrelation, finding it similar to the one in M 13, a possible indication of a relation with HB morphology. However, the degree of chemical anomalies is not as severe as that in M 13. Further light on the subject is expected once we have completed the analysis of our GC survey, covering the whole range of cluster physical parameters.

Acknowledgements. We thank Dr. D. Yong for providing unpublished *EW*s. This publication makes use of data products from the Two Micron All Sky Survey, which is a joint project of the University of Massachusetts and the Infrared Processing and Analysis Center/California Institute of Technology, funded by the National Aeronautics and Space Administration and the National Science Foundation. This work was partially funded by the Italian MIUR under PRIN 2003029437. We also acknowledge partial support from the grant INAF 2005 "Experimental nucleosynthesis in clean environments".

References

Alonso, A., Arribas, S., & Martinez-Roger, C. 1999, A&AS, 140, 261
Alonso, A., Arribas, S., & Martinez-Roger, C. 2001, A&A, 376, 1039
Asplund, M. 2005, ARA&A, 43, 481
Bragaglia, A., Carretta, E., Gratton, R. G., et al. 2001, AJ, 121, 327
Brown, J. H., Burkert, A., & Truran, James W. 1991, ApJ, 376, 115
Brown, J. H., Burkert, A., & Truran, James W. 1995, ApJ, 440, 666
Buonanno, R., Caloi, V., Castellani, V., et al. 1986, A&AS, 66, 79
Buzzoni, A., Fusi Pecci, F., Buonanno, R., & Corsi, C. E. 1983, A&A, 128, 94
Cardelli, J. A., Clayton, G. C., & Mathis, J. S. 1989, ApJ, 345, 245
Carretta, E. 1994, Ph.D. Thesis, University of Padova
Carretta, E. 2006, AJ, 131, 1766
Carretta, E., & Gratton, R. G. 1997, A&AS, 121, 95
Carretta, E., Gratton R. G., Lucatello, S., Bragaglia, A., & Bonifacio, P. 2005, A&A, 433, 597
Carretta, E., Bragaglia, A., Gratton, R. G., et al. 2006, A&A, 450, 523 (Paper I)
Cayrel, R. 1986, A&A, 168, 8
Cohen, J. G., & Melendez, J. 2005, AJ, 129, 303
D'Antona, F., & Caloi, V. 2004, ApJ, 611, 871
Denisenkov, P. A., & Denisenkova, S. N. 1989, A.Tsir., 1538, 11
Gratton, R. G., Carretta, E., Eriksson, K., & Gustafsson, B. 1999, A&A, 350, 955
Gratton, R. G., Sneden, C., Carretta, E., & Bragaglia, A. 2000, A&A, 354, 169
Gratton, R. G., Bonifacio, P., Bragaglia, A., et al. 2001, A&A, 369, 87
Gratton, R. G., Bragaglia, A., Carretta, E., et al. 2003a, A&A, 408, 529
Gratton, R. G., Carretta, E., Claudi, R., Lucatello, S., & Barbieri, M. 2003b, A&A, 404, 187
Gratton, R. G., Sneden, C., & Carretta, E. 2004, ARA&A, 42, 385
Gratton, R. G., Bragaglia, A., Carretta, E., et al. 2005, A&A, 440, 901
Grundahl, F., Briley, M., Nissen, P. E., & Feltzing, S. 2002, A&A, 385, L14
Harris, W. E. 1996, AJ, 112, 1487
Kraft, R. P. 1994, PASP, 106, 553
Kurucz, R. L. 1993, CD-ROM 13, Smithsonian Astrophysical
Langer, G. E., Hoffman, R., & Sneden, C. 1993, PASP, 105, 301
Magain, P. 1984, A&A, 134, 189
Momany, Y., Bedin, L. R., Cassisi, S., et al. 2004, A&A, 420, 605
Moni Bidin, C., Moehler, S., Piotto, G., et al. 2006, A&A, 451, 499
Norris, J. E., & Da Costa, G. S. 1995, ApJ, 441, L81
Parmentier, G., & Gilmore, G. 2001, A&A, 378, 97
Pasquini, L., Avila, G., Blecha, A., et al. 2002, The Messenger, 110, 1
Prantzos, N., & Charbonnel, C. 2006, A&A, 458, 135
Pritzl, B. J., Venn, K. A., & Irwin, M. 2005, AJ, 130, 2140
Ramirez, S., & Cohen, J. G. 2003, AJ, 125, 224
Rosenberg, A., Saviane, I., Piotto, G., & Aparicio, A. 1999, AJ, 118, 2306
Sandquist, E. L. 2000, MNRAS, 313, 571
Skrutskie, M. F., Cutri, R. M., Stiening, R., et al. 2006, AJ, 131, 1163
Sneden, C., Kraft, R. P., Guhathakurta, P., Peterson, R. C., & Fulbright, J. P. 2004, AJ, 127, 2162
Ventura, P. D'Antona, F., Mazzitelli, I., & Gratton, R. 2001, ApJ, 550, L65
Yong, D., Grundahl, F., Lambert, D. L., Nissen, P. E., & Shetrone, M. D. 2003, A&A, 402, 985
Yong, D., Grundahl, F., Nissen, P. E., Jensen, H. R., & Lambert, D. L. 2005, A&A, 438, 875